

See discussions, stats, and author profiles for this publication at: <https://www.researchgate.net/publication/5855606>

# Identification of Ritual Blood in African Artifacts Using TOF-SIMS and Synchrotron Radiation Microspectroscopies

ARTICLE *in* ANALYTICAL CHEMISTRY · DECEMBER 2007

Impact Factor: 5.64 · DOI: 10.1021/ac070993k · Source: PubMed

CITATIONS

37

READS

9

8 AUTHORS, INCLUDING:



**Vincent Mazel**

University of Bordeaux

38 PUBLICATIONS 245 CITATIONS

SEE PROFILE



**Delphine Debois**

ZenTech S.A.

26 PUBLICATIONS 546 CITATIONS

SEE PROFILE



**David Touboul**

Natural Product Chemistry Institute

118 PUBLICATIONS 2,008 CITATIONS

SEE PROFILE



**Olivier Lapr v te**

Universit  Ren  Descartes - Paris 5

245 PUBLICATIONS 4,184 CITATIONS

SEE PROFILE

## Articles

# Identification of Ritual Blood in African Artifacts Using TOF-SIMS and Synchrotron Radiation Microspectroscopies

Vincent Mazel,<sup>†,‡</sup> Pascale Richardin,<sup>\*,†</sup> Delphine Debois,<sup>‡</sup> David Touboul,<sup>‡,‡</sup> Marine Cotte,<sup>†,§</sup> Alain Brunelle,<sup>‡</sup> Philippe Walter,<sup>†</sup> and Olivier Laprévote<sup>‡</sup>

Centre de Recherche et de Restauration des Musées de France (C2RMF), CNRS UMR 171, Palais du Louvre, Porte des Lions, 14, quai François Mitterrand, 75001 Paris, France, Laboratoire de Spectrométrie de Masse, Institut de Chimie des Substances Naturelles, CNRS UPR 2301, Avenue de la Terrasse, 91198 Gif-sur-Yvette, France, and European Synchrotron Research Facility, 6 rue Jules Horowitz, BP220, 38043 Grenoble cedex, France

A new protocol is implemented to demonstrate the presence of blood in the patina of African art objects from Mali. Divided into three steps, the protocol first consists in demonstrating the presence of proteins and localizing them in the sample's cross sections using time-of-flight secondary ion mass spectrometry (TOF-SIMS) and synchrotron-based infrared microspectrometry ( $\mu$ FT-IR). In a second time, TOF-SIMS is used to investigate heme, which is a blood marker. If heme is missing, which could mean that it is too degraded to be detected, X-ray microfluorescence ( $\mu$ XRF) and X-ray absorption near-edge microspectroscopy ( $\mu$ XANES) are used to prove the presence of iron in the protein area and to get a fingerprint of its chemical environment. This permits us thus to demonstrate that iron is indeed linked with proteins and not with mineral phases of the sample. Coupled with the ritual context of the objects, this constitutes a proof of the use of blood. Thanks to this protocol, which has the major advantage of avoiding false positive results, the presence of blood has been demonstrated in seven out of the eight studied samples.

African art objects collected in the course of colonial or ethnological expeditions during the 20th century represent unique and very precious material testimony of values and practices, which have in some cases totally disappeared today. Numbers of these objects, which are now parts of the collections of art or ethnologic museums, are partially or completely covered with a so-called "patina". Indeed, different substances were spread out

on the objects during religious and ritual ceremonies.<sup>1</sup> Various examples of such patinas in African statuary come from different ethnic groups like the Baoule in Ivory Coast,<sup>1</sup> Lobi in Burkina-Faso,<sup>2</sup> Fang in Gabon, but also Bambara and Dogon in Mali.<sup>3,4</sup> Some of these patinas are constituted by materials which have become solid on the object's surface, like a more or less thick crust.

The bibliographic references come from ethnologic studies, such as the very important work of Marcel Griaule<sup>5,6</sup> who has collected a large number of ritual objects associated with very precious accounts about traditional beliefs of the Dogon. A better understanding of these patinas could explain details of the practices used during centuries throughout ceremonies. An important challenge is to extract unequivocal information about the original constituents of these patinas and the techniques used for their applications on ritual objects. Many substances are used, each product having its religious meaning and importance. Among these, blood is often reported in different religious contexts,<sup>7,8</sup> linked to animal sacrifices. Confirmation of the presence of blood would be very meaningful.

In a previous paper, we described an original analytical protocol based on chemical imaging techniques to study patinas from African statues.<sup>9</sup> The protocol permitted us to study both the mineral and the organic parts of a sample without extraction of

\* Corresponding author. Phone: +33 (0) 1 40 20 24 65. E-mail: pascale.richardin@culture.gouv.fr.

<sup>†</sup> Centre de Recherche et de Restauration des Musées de France.

<sup>‡</sup> Institut de Chimie des Substances Naturelles.

<sup>§</sup> European Synchrotron Research Facility.

<sup>‡</sup> Present address: Laboratoire Matériaux et Santé (EA 401), Faculté de pharmacie de Châtenay Malabry, 5 rue Jean-Baptiste Clément, 92296 Châtenay-Malabry.

<sup>‡</sup> Present address: Department of Chemistry and Applied Biosciences, ETH Zürich, CH-8093 Zürich, Switzerland.

(1) Cornec, S. *Technè* 2000, 11, 40–45.

(2) Bogniolo, D. In *Images d'Afrique Noire et Sciences Sociales: les pays Lobi, Birifor et Dagara (Burkina Faso, Côte-d'Ivoire et Ghana)*; Fiéloux, M., Lombard, J., Kambou-Ferrand, J.-M., Eds.; Karthala-Orstom: Paris, 1993; pp 379–396.

(3) Leloup, H.; Rubin, W.; Serra, R.; BASELITZ, G. *Statuaire Dogon*; Danièle Ameiz: Strasbourg, 1994.

(4) Bedaux, R.; Person, A. In *Regards sur les Dogon du Mali*; Bedaux, R., Van der Waals, J. D. Eds.; Editions Snoeck: Gent, Belgium, 2003; pp 128–133.

(5) Griaule, M. *Journal de la Société des Africanistes (Paris)* 1932, II, 113–122.

(6) Griaule, M., *Journal de la Société des Africanistes (Paris)* 1932, II, 229–236.

(7) Brett-Smith, S. *Anthrop. Aesthetics* 1983, 6, 47–63.

(8) Ndiaye, F.; Calame-Griaule, G.; Martinelli, B. *L'art Dogon dans les Collections du Musée de l'Homme*; Museum Rietberg: Zürich, Switzerland, 1995.

(9) Mazel, V.; Richardin, P.; Touboul, D.; Brunelle, A.; Walter, P.; Laprévote, O. *Anal. Chim. Acta* 2006, 570, 34–40.

the compounds. This approach has the great advantage of being nondestructive for the sample, allowing further analyses to be performed. This feature is very important in the field of cultural heritage because of restricted sampling. The present research follows a similar approach<sup>9</sup> but focuses on the detection of blood in patinas. It aims at showing the possibility, via multitechnical and nondestructive analyses, to demonstrate the presence of blood.

Since the beginning of the 1980s, a large number of articles have been published about blood identification in cultural heritage artifacts. In most cases, they concern the analysis of prehistoric objects, e.g., stone tools or prehistoric paintings. In these studies we can distinguish two kinds of approaches. The first is based on various immunological tests, in which blood immunological properties are involved.<sup>10–13</sup> This process is very powerful, because it can lead to the identification of the species at the origin of the blood. However, its reliability is still controversial.<sup>14–18</sup> In a second approach, blood is identified by showing the presence of hemoglobin or hemoglobin markers such as heme or red blood cells. For that purpose, a lot of different techniques are used, like optical microscopy,<sup>19</sup> electron microscopy,<sup>20</sup> liquid chromatography,<sup>21,22</sup> and colorimetric tests.<sup>12,23</sup> With these kinds of tests, it is not possible to identify the origin of the blood.

Each sample has been first examined by scanning electron microscopy coupled with elemental analysis. Results have shown that they are mostly composed of organic matter with some inorganic phases, consisting of aluminosilicates and calcium carbonates.<sup>24</sup> In only one case out of more than 10 samples, red blood cells have been observed,<sup>25</sup> demonstrating the presence of blood in this patina without ambiguity. These structures are nevertheless not always well preserved, and the observation of red blood cells in a unique sample does not mean that blood is missing in other samples. We therefore decided to develop a new protocol for the identification of blood.

## ANALYTICAL STRATEGY

The following protocol, based on the combination of several techniques, has been developed, on the basis of the existing literature and keeping in mind the choice of working without any extractive method: time-of-flight secondary ion mass spectrometry (TOF-SIMS) together with techniques based on synchrotron

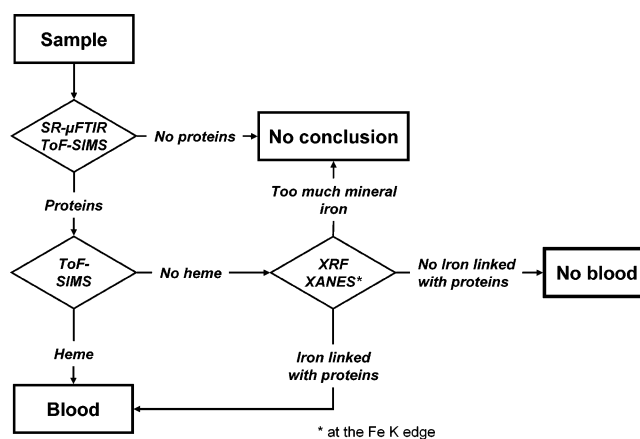


**Figure 1.** Schematic view of the analytical strategy developed for blood identification.

radiation, infrared microscopy (SR-μFT-IR), X-ray microfluorescence (μXRF), and X-ray absorption near-edge microspectroscopy (μXANES). Using these methods, we investigated hemoglobin features and more precisely the occurrence of heme and iron bound with proteins. These three different techniques have been chosen because they are complementary and because of their ability to work on microsamples in a noninvasive way. This last point is essential when working on cultural heritage artifacts.

The strategy is divided into three steps. The first step consists of probing the presence of proteins using both SR-μFT-IR and TOF-SIMS. Indeed, proteins constitute the main part of dried blood. If they are not detected, it means that either blood is not present or blood proteins are fully degraded. Consequently, another analytical strategy has to be implemented.

At the opposite, if proteins are present, TOF-SIMS is used for the identification of the heme group, which is a blood marker. It is well-known that heme can undergo degradation phenomena due to its environmental conditions.<sup>26</sup> So a lack of heme could mean either that proteins do not come from blood or that heme is degraded. This case leads to the third step: iron is probed by μXRF, particularly in regions containing proteins. The occurrence of iron within proteins, coupled with the ritual context of the objects, would constitute a solid proof.

As iron-containing minerals may also be present in the patina, μXRF measurements are coupled with μXANES analyses in order to get a fingerprint of the iron environment in the sample. This will help us distinguishing between iron coming from a mineral phase and iron coming from blood.

This entire approach is summarized in Figure 1.

## EXPERIMENTAL SECTION

**Samples.** The objects studied belong to the collections of the Musée du Quai Branly, Paris, France. The patinas of eight objects from Mali have been analyzed. Among them, three are ritual objects from the Dogon culture. The five other artifacts are *boliv* (in the singular: *boliv*), which are among the most important sacred objects from the Bamana culture.<sup>7</sup> All these artifacts have been collected in the first half of the 20th century during ethnological missions, except one of the *boliv* (inventory no. 73.1967.6.1) which

- (10) Newman, M. E.; Yohe, R. M., II; Ceri, H.; Sutton, M. Q. *J. Archaeol. Sci.* **1993**, *20*, 93–100.
- (11) Tuross, N.; Barnes, I.; Potts, R. *J. Archaeol. Sci.* **1996**, *23*, 289–296.
- (12) Williamson, B. S. *J. Archaeol. Sci.* **2000**, *27*, 755–762.
- (13) Lowenstein, J. M.; Reuther, J. D.; Hodd, D. G.; Scheuenstuhl, G.; Gerlach, S. C.; Ubelaker, D. H. *Forensic Sci. Int.* **2006**, *159*, 182–188.
- (14) Eisele, J. A.; Fowler, D. D.; Haynes, G.; Lewis, R. A. *Antiquity* **1995**, *69*, 36–46.
- (15) Leach, J. D.; Mauldin, R. P. *Antiquity* **1995**, *69*, 1020–22.
- (16) Fiedel, S. J. *J. Archaeol. Sci.* **1996**, *23*, 139–147.
- (17) Newman, M. E.; Ceri, H.; Kooyman, B. *Antiquity* **1996**, *70*, 677–82.
- (18) Newman, M. E.; Yohe, R. M., II; Kooyman, B.; Ceri, H. *J. Archaeol. Sci.* **1997**, *24*, 1023–1027.
- (19) Loy, T. H. *Science* **1983**, *220*, 1269–1271.
- (20) Hortola, P. *J. Archaeol. Sci.* **2002**, *29*, 733–739.
- (21) Loy, T. H.; Hardy, B. L. *Antiquity* **1992**, *66*, 24–35.
- (22) Schweitzer, M. H.; Marshall, M.; Carron, K.; Bohle, D. S.; Busse, S. C.; Arnold, E. V.; Barnard, D.; Horner, J. R.; Starkey, J. R. *Proc. Natl. Acad. Sci. U.S.A.* **1997**, *94*, 6291–6296.
- (23) Gurfinkel, D. M.; Franklin, U. M. *J. Archaeol. Sci.* **1988**, *15*, 83–97.
- (24) Mazel, V.; Richardin, P. *Technè* **2006**, *23*, 69–73.
- (25) Mazel, V.; Richardin, P.; Charlier, P. *Actes du 1er Colloque International de Pathologie*, 2005, pp 131–144.
- (26) Hiroyuki, I.; Fukutaro, T.; Mineo, I.; Yoshitaka, M.; Yoshimi, S. *Forensic Sci. Int.* **1992**, *57*, 17–27.

**Table 1. List of the Samples**

sample	ethnic origin of the object	object inventory no.	object type
D1	Dogon	71.1935.105.169	anthropomorphic statuette
D2	Dogon	71.1935.60.332	anthropomorphic statuette
D3	Dogon	71.1935.01.156	anthropomorphic statuette
B1	Bamana	71.1931.74.1091	zoomorphic object (boli)
B2	Bamana	73.1967.6.1	zoomorphic object (boli)
B3	Bamana	71.1902.12.10	composite object (boli)
B4	Bamana	71.1910.1.93	composite object (boli)
B5	Bamana	71.1902.10.15.1-2	composite object (boli)

was bought in 1967 by the former Musée des Arts d'Afrique et d'Océanie, Paris. These objects can be dated from the end of the 19th century or the beginning of the 20th century, except the Dogon sculpture (inventory no. 71.1935.105.156) which could be much older (12th to 14th century).

The Dogon artifacts are anthropomorphic wooden statuettes. Two of them are covered with a heterogeneous layer of patina (inventory no. 71.1935.60.332; inventory no. 71.1935.105.169), whereas the third one (inventory no. 71.1935.105.156) is more homogeneous. Concerning the boliw, two artifacts have a zoomorphic shape made of a structure of bamboo (inventory no. 71.1931.74.1091; inventory no. 73.1967.6.1), whereas the others are made of wood with different shapes (inventory no. 71.1902.12.10; inventory no. 71.1910.1.93; inventory no. 71.1902.10.15.1-2). All of them are covered with a very thick black layer of patina.

Microsamples were removed from the surface of the objects with a clean scalpel blade. In the text the eight studied samples will be named as described in Table 1.

Standard samples of hemin, Zn (II)–protoporphyrin IX, protoporphyrin IX, and bovine hemoglobin were purchased from Sigma-Aldrich (St Quentin Fallavier, France).

**Sample Preparation.** Preparation of cross sections of the samples has already been described elsewhere.<sup>9</sup> The sample is embedded in a polyester resin (H59 Sodemi, France). The block is then cut by ultramicrotomy using a Diatome diamond knife (Leica Microsystems, France) until reaching the core of the sample. All the measurements are then performed on the flat and clean exposed surface.

**Time-of-Flight Secondary Ion Mass Spectrometry.** TOF-SIMS analyses were performed on a TOF-SIMS IV (ION-TOF GmbH, Münster, Germany) reflectron-type TOF mass spectrometer. The primary ion source was a bismuth liquid metal ion gun. A 25 keV Bi<sub>3</sub><sup>+</sup> ion beam was selected with an incidence angle of 45° in the so-called high-current bunched mode.<sup>27,28</sup> This ion source operating mode ensures both a 1–2 μm primary ion beam focus and a high mass resolution ( $M/\Delta M = 10^4$  [full width at half-maximum, fwhm] at  $m/z$  500), which is a prerequisite for accurate mass measurements and assignments. Each image was acquired with a primary ion dose density (= fluence) of 10<sup>11</sup> ions·cm<sup>-2</sup> and a lateral resolution of 2 μm. Secondary ions are extracted with 2 kV voltage and are postaccelerated to 10 keV kinetic energy just before hitting the detector surface.

During the measurement, the TOF mass spectrum was recorded over the area of each pixel. This allows, on the one hand,

drawing the spatial distribution of any compound detected at the surface of the sample and, on the other hand, reconstructing the spectrum of any area of the image. All images shown in this paper are normalized to the total ion current.

**Techniques Using Synchrotron Radiation.** All the experiments based on synchrotron radiation were performed at the FT-IR and X-ray microscopes of the ID21 beam line, ESRF, Grenoble, France.

**FT-IR Microscopy.** FT-IR microscopy was performed on the ID21-infrared end station.<sup>29</sup> The instrument is a Nexus spectrometer coupled with a confocal Continuum microscope, from Nicolet. All measurements were performed in specular reflectance mode, with backgrounds acquired on a gold mirror. Thanks to the high brightness of the synchrotron source, the spot size could be reduced to 12 μm × 12 μm, which was a good tradeoff between lateral resolution and flux. An accumulation of 40 scans was enough to obtain a signal-to-noise ratio of about 2 × 10<sup>5</sup>. Two-dimensional (2D) mapping was performed with a step of 10 μm in each direction, in order to draw chemical image of the vibration bands detected.

**Micro-X-ray Fluorescence and XANES.** Elemental maps were obtained using the ID21 scanning X-ray microscope. Briefly, the fluorescence excitation is stimulated with a highly monochromatic beam by means of a fixed-exit double-crystal Si (111) monochromator, with a tunable energy ranging from 2.1 to 7.2 keV. For the micro-X-ray fluorescence mapping, the excitation energy was set to 7.2 keV, which is just above the first ionization energy of iron and is very suitable for its detection. Experiments were done under vacuum to improve sensitivity by minimizing absorption and scattering from air. Analyses were performed with a spot size of approximately 0.4 μm × 1.2 μm, obtained thanks to Fresnel zone plates. The microfluorescence signal was collected in the horizontal plane perpendicular to the incident beam direction by using a HPGe solid-state energy-dispersive detector. The detailed setup is described elsewhere.<sup>30</sup>

Areas of 95 μm × 95 μm were mapped on the samples with a step size of 1 μm in each direction. It is then possible to draw the elemental maps, i.e., the spatial distribution of each detected element.

In order to characterize the iron molecular environment, the absorption was measured while tuning the energy of the probing X-ray photons across the Fe K edge. The spectral features observed, namely, the XANES, offer information on iron speciation (oxidation state and coordination).

Measurements were performed in fluorescence mode with an incident energy ranging from 7.1 to 7.3 keV in steps of 0.2 eV and a dwell time of 2 s. The resolution of the monochromator is 0.7 eV and the calibration was performed on an iron foil. Thirty spectra were accumulated for each of the points chosen on the chemical image of iron obtained by XRF.

## RESULTS AND DISCUSSION

**Localization of Proteins.** Intact proteins cannot be detected by TOF-SIMS, but low  $m/z$  characteristic fragments can be

(27) Sodhi, R. N. S. *Analyst* **2004**, *129*, 483–487.

(28) Brunelle, A.; Touboul, D.; Laprévotte, O. *J. Mass Spectrom.* **2005**, *40*, 985–999.

(29) Susini, J.; Cotte, M.; Scheidt, K.; Chubar, O.; Polack, F.; Dumas, P. *Synchrotron Radiat. News* **2007**, in press.

(30) Susini, J.; Salomé, M.; Fayard, B.; Ortega, R.; Kaulich, B. *Surf. Rev. Lett.* **2002**, *9*, 203–211.



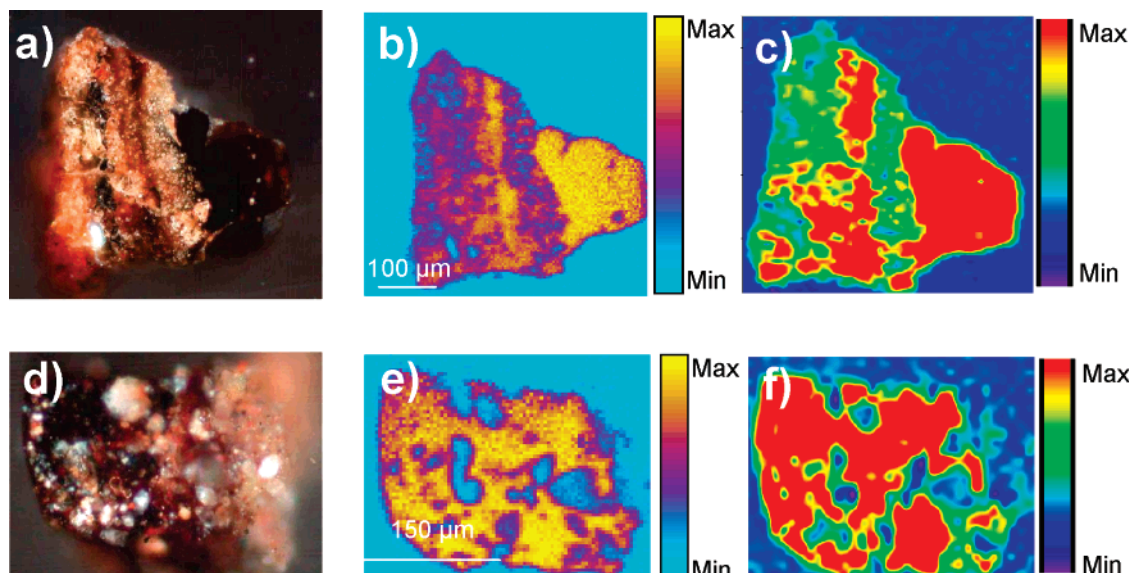


**Figure 2.** Localization of proteins. Sample D1: (a) microscopic view of the cross section, (b) TOF-SIMS spatial distribution of the proteins (sum of amino acids fragments), and (c) infrared image of the amide I band of proteins. Sample B2: (d) microscopic view of the cross section, (e) TOF-SIMS spatial distribution of the proteins (sum of amino acids fragments), and (f) infrared image of the amide I band of proteins.

**Table 2.  $m/z$  Values Attribution of the Principal Amino Acid Fragments Used for Proteins Characterization and Localization**

$m/z$	ion	amino acid
30.03	$\text{CH}_4\text{N}^+$	glycine
44.05	$\text{C}_2\text{H}_6\text{N}^+$	alanine
70.06	$\text{C}_4\text{H}_8\text{N}^+$	proline
72.08	$\text{C}_4\text{H}_{10}\text{N}^+$	valine
84.08	$\text{C}_5\text{H}_{10}\text{N}^+$	lysine
86.09	$\text{C}_5\text{H}_{12}\text{N}^+$	leucine/isoleucine
110.07	$\text{C}_5\text{H}_8\text{N}_3^+$	histidine
120.08	$\text{C}_8\text{H}_{10}\text{N}^+$	phenylalanine
130.06	$\text{C}_9\text{H}_8\text{N}^+$	tryptophan

observed<sup>31,32</sup> (Table 2). The presence of proteins is assessed thanks to the correlation between all the 2D images of these various fragments.<sup>9</sup> Images of the different ions are then added up to increase the signal-to-noise ratio, and the resulting image gives the distribution of the proteins in the sample. Examples of samples D1 and B2 are shown on Figure 2, parts b and e.

To confirm this attribution and localization, the image obtained with SR- $\mu$ FT-IR is correlated with the TOF-SIMS one. The amide I band is chosen to draw the protein image (Figure 2, parts c and f). If the two techniques lead to the same distribution, the presence of proteins as well as their spatial distribution are definitively confirmed.

In all the eight samples, proteins were attributed and located by this way. The investigation process was followed by the characterization of heme by TOF-SIMS.

**Characterization of Heme by TOF-SIMS.** Heme (MW 616.18) is a complex between an iron ion and a protoporphyrin IX. It is bound to hemoglobin and is responsible of oxygen carriage in organism.

We first studied hemin, Fe(III)–protoporphyrin IX chloride, which is the only commercially available form of heme. Positive ionization mode was found to be the most suitable to analyze this product. The spectrum displayed in Figure 3b shows two main features. First, peaks around  $m/z$  616, with a major peak at  $m/z$  616.2, can be identified as unfragmented heme ions. The isotopic patterns of  $[\text{M}]^+$  and  $[\text{M} + \text{H}]^+$  ions are overlapping in the spectra. As hemin is a heme chloride, iron should be present as Fe(III), leading to  $[\text{M}]^+$  ion, which is indeed the predominant ion.  $[\text{M} + \text{H}]^+$  ion comes from Fe(II)<sup>33</sup> which can be present as an impurity in the sample or also produced during the ionization process.

Between  $m/z$  350 and  $m/z$  550 a large distribution of peaks centered at  $m/z$  480 with a Gaussian-like shape is detected. This distribution is complex and composed of smaller peak distributions separated by 14 amu, which indicates that they arise from the fragmentation of the porphyrin. A test made using the PSD-like mode<sup>34</sup> on the unfragmented ions does not show these kinds of fragments, which means that they are formed in the source, where the processes are more energetic than in the analyzer part. Previous studies in chemical ionization mass spectrometry have shown that the fragmentation of the porphyrin macrocycle was possible and leads to mono-, di-, and tripyrroles fragments.<sup>35–37</sup> According to the mass range, the fragments observed in the spectra of Figure 3 could be assigned to tripyrroles ions.

To ensure these interpretations, spectra of Zn(II)–protoporphyrin IX and metal-free protoporphyrin IX were acquired. For the Zn(II)–protoporphyrin IX, a similar spectrum is obtained

(31) Sanni, O. D.; Wagner, M. S.; Briggs, D. G.; Castner, D. G.; Vickerman, J. C. *Surf. Interface Anal.* **2002**, *33*, 715–728.

(32) Wagner, M. S.; Castner, D. G. *Appl. Surf. Sci.* **2004**, *231–232*, 366–376.

(33) Chiavarino, B.; Crestoni, M. E.; Fornarini, S.; Rovira, C. *Chem. Eur. J.* **2007**, *13* (3), 776–785.

(34) Touboul, D.; Brunelle, A.; Laprévote, O. *Rapid Comm. Mass Spectrom.* **2006**, *20*, 703–709.

(35) Shaw, G. J.; Eglinton, G.; Quirke, J. M. E. *Anal. Chem.* **1981**, *53* (13), 2014–2020.

(36) Tolf, B. R.; Jiang, X. Y.; Wegmann-Szente, A.; Kehres, L. A.; Bunnenberg, E.; Djerassi, C. *J. Am. Chem. Soc.* **1986**, *108* (7), 1363–1374.

(37) Van Berkel, G. J.; Glish, G. L.; McLuckey, S. A.; Tuinman, A. A. *J. Am. Chem. Soc.* **1989**, *111* (16), 6027–6035.

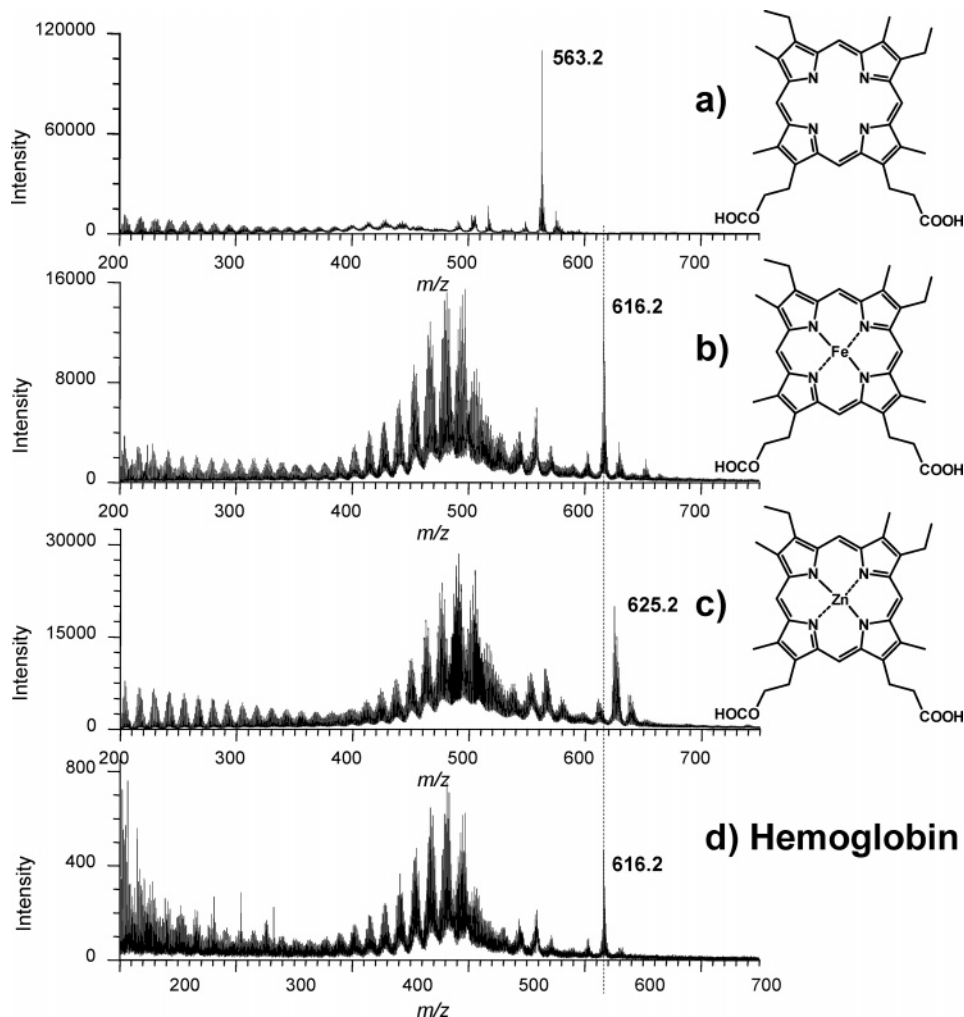


**Figure 3.** TOF-SIMS spectra of porphyrin standards and hemoglobin: (a) protoporphyrin IX, (b) hemin, (c) Zn(II)–protoporphyrin IX, and (d) hemoglobin.

(Figure 3c) with the unfragmented ions and the large distribution of fragments. Yet, two differences can be noted. First, the major unfragmented ion is  $[M + H]^+$  at  $m/z$  625.2, corresponding to Zn(II), as expected for this product. Then, the  $m/z$  ratio of the fragments is shifted to higher  $m/z$  values. The only chemical difference between this product and hemin being the metal ion, we can conclude that metal ions are present in the fragments. Nevertheless, the mass shift is approximately 10 amu instead of 8 or 9 amu as expected. This difference could be due to isotopic pattern of Zn and Fe but the complexity of the peaks distribution makes it difficult to verify.

The fragment distribution of the metal-free protoporphyrin IX was also obtained (Figure 3a) but is much less intense and shifted to lower mass values due to the absence of the metal ion. This means that the fragmentation of the porphyrin macrocycle is favored by the presence of the metal ion.

This analysis of standards has demonstrated that TOF-SIMS allows detecting heme thanks to the unfragmented peaks and the distribution of metal-containing fragments, which is confirmed in the spectrum of hemoglobin (Figure 3d). It is thus well-known that heme undergoes degradation due to environmental conditions.<sup>26</sup> We cannot therefore ensure that, even if blood is present, the remaining amount of heme in our samples is sufficient to be

detected. Within the eight samples, three different cases were observed.

The first case corresponds to sample B3 (Figure 4a). The recorded spectrum clearly shows all the features of heme, which can be identified with no doubt. Moreover, Figure 4a shows that the spatial distribution of heme corresponds to the one of proteins. We can conclude that this sample, and most generally the patina of the object inventory no. 71.1902.12.10, is composed, at least for a part, of blood.

The second case concerns samples B1, B2, and B5. Spectra obtained by TOF-SIMS still show the characteristic peaks of heme, and heme displays the same spatial distribution as proteins (Figure 4b). Nevertheless, we obtain a much lower signal-to-noise ratio which means that the amount of heme is much lower than in the previous case. Heme is probably more degraded. However, the quantity is still sufficient to be detected by TOF-SIMS and the conclusion is, here also, that blood is present in these samples.

Finally no heme is detected for samples D1, D2, D3, and B4. The limits of blood identification by TOF-SIMS may have been reached; either proteins do not belong to blood, or degradation of heme is too important. Another approach is necessary to confirm or not the lack of blood. Of course, if there is blood, and

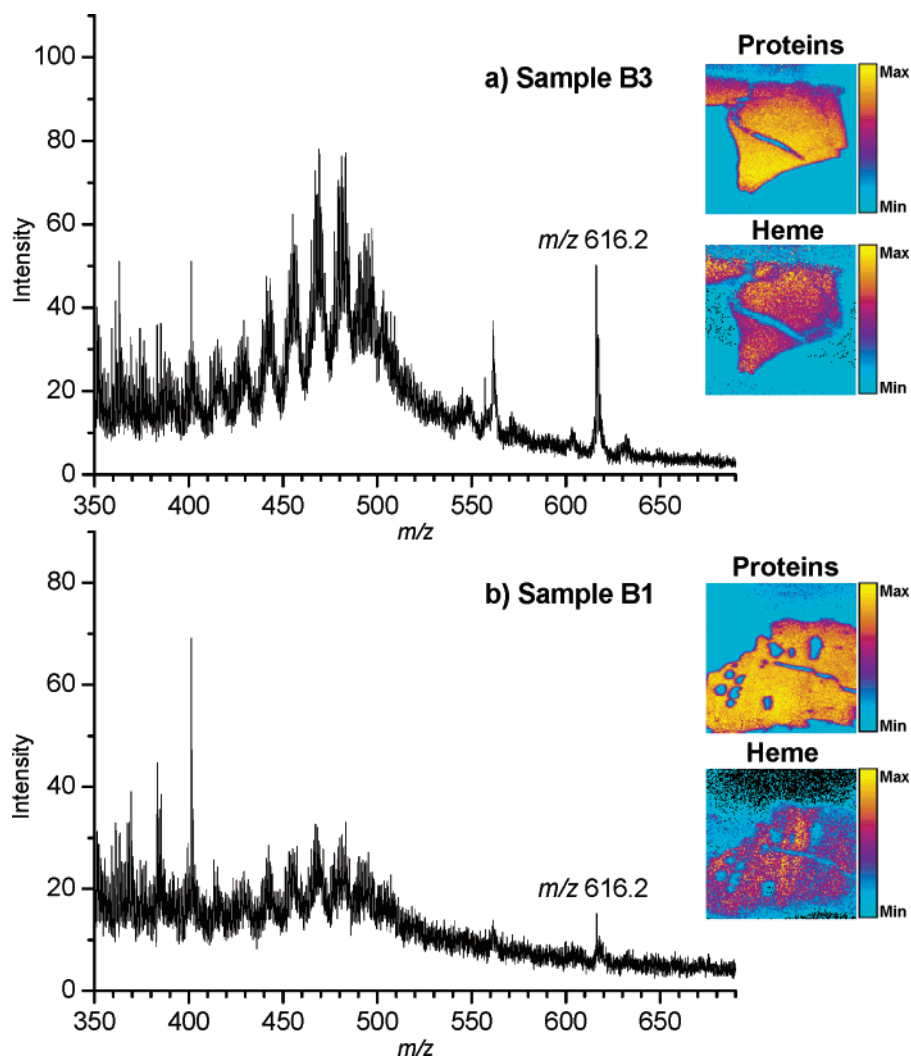


**Figure 4.** TOF-SIMS study of two samples: detail of spectrum and spatial distribution of proteins (sum of amino acids fragments) and heme (tripyrrole fragments) for (a) sample B3 and (b) sample B1.

heme is no longer present, iron should still be detectable in the proteins.

**Iron in the Proteins:  $\mu$ -XRF and  $\mu$ -XANES Study.** On each sample, an area where proteins were detected by  $\mu$ -FT-IR and by TOF-SIMS was first analyzed by XRF.

Contrary to ion beams or infrared radiations, which only probe the surface of the sample (secondary ions are emitted from a depth of less than 10 nm for TOF-SIMS, and a depth of a few micrometers is analyzed for SR-FT-IR), X-rays collect deeper information in the matter, reaching the core of the sample. Care must thus be taken when comparing results from these different techniques. Samples may be also composed of a mineral part, consisting mainly of clays, which may contain iron, at least as an impurity. If iron is detected, it can therefore belong to clays underlying the proteins located at the surface. As the energy used provides a low efficiency of fluorescence for low  $Z$  elements, silicon and aluminum from the clay may not be detected if located in deep layers far below the surface.

The discrimination between iron from mineral and organic matter can first be done with a simple argument. In iron-containing proteins, the spatial distribution of this metal should be homogeneous. To the contrary the distribution of iron in clays

underneath the surface should be inhomogeneous when observed by XRF, because clays generally exhibit a shape of microscopic grains.

Figure 5b shows the chemical image of iron in a protein-rich area for sample D1. Both homogeneous (center) and heterogeneous areas (sides) can be distinguished in the image. This proves that the iron signal detected in the central part of the image (Figure 5c) comes from the proteins. Similar results have been obtained for samples D2 and B4. On the contrary, for sample D3, no homogeneous areas can be observed, which means that inorganic compounds may be present beneath the whole surface protein layer.

In order to confirm this interpretation, XANES experiments at the Fe K edge were performed to obtain a fingerprint of iron environment in the sample. Several measurements were done at different points corresponding to the different areas of the image. All the spectra were normalized to 1, far after the edge, to facilitate the comparison. Two different cases were observed.

In the proteins area, a photoreduction phenomenon occurs under the X-ray beam, and the absorption threshold moves to a lower energy during the experiment (Figure 5d). This phenomenon is already well-known for organic materials and more

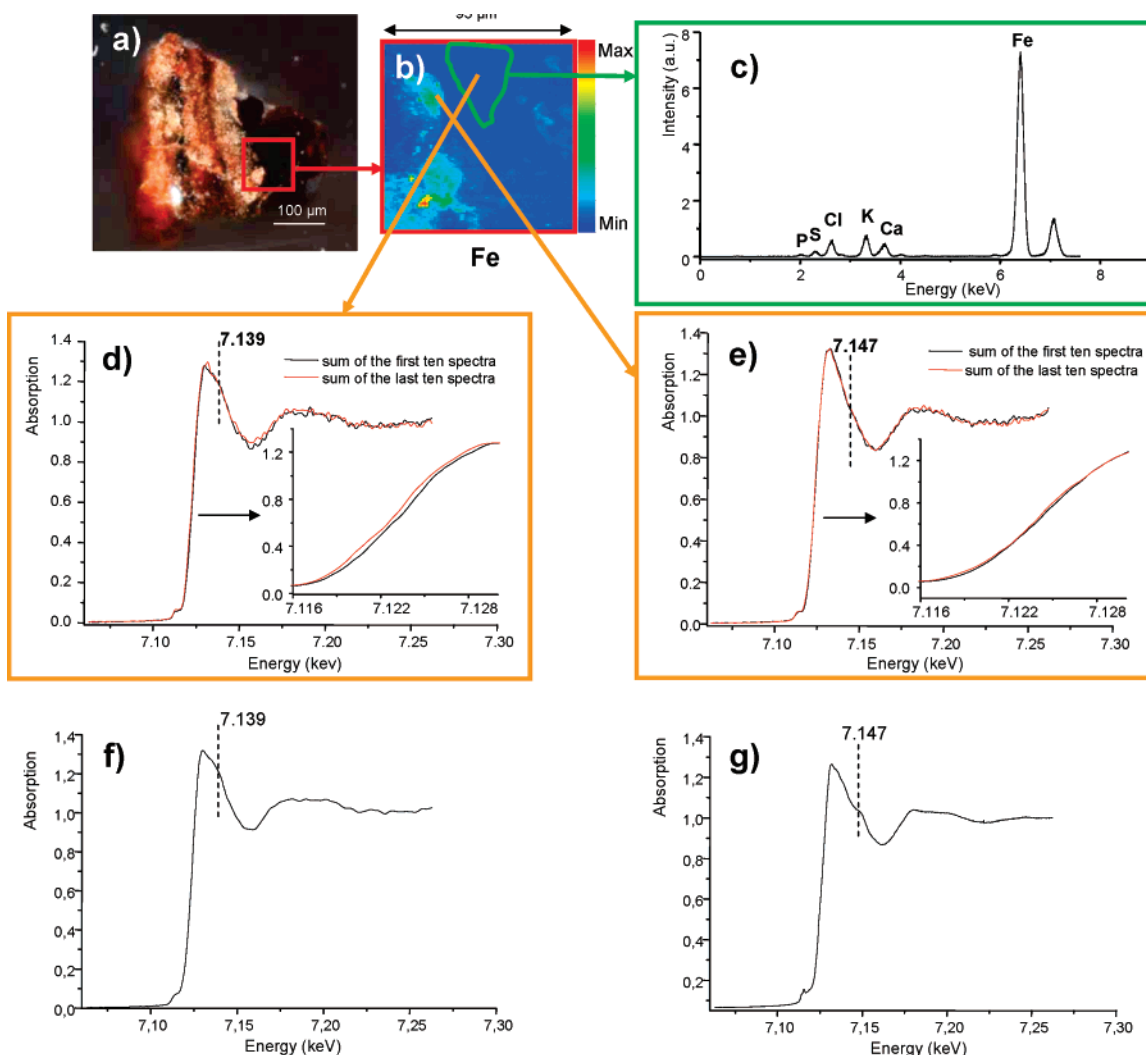


**Figure 5.** XRF and XANES analysis of sample D1: (a) microscopic view of the sample. The analyzed area is surrounded in red; (b) XRF image of iron; (c) spectrum of the central area; (d) evolution of XANES spectrum for so-supposed organic area; (e) evolution of XANES spectrum for inorganic area; (f) reference spectrum of hemoglobin; (g) reference spectrum of goethite.

precisely for the analysis of blood by EXAFS (extended X-ray absorption fine structure) and XANES.<sup>38,39</sup> Moreover, all these spectra present a little hump at approximately 7.139 keV which can also be observed on hemoglobin reference spectrum (Figure 5f).

For the area where mineral compounds are supposed to be predominant, this evolution is not observed (Figure 5e). All the recorded spectra present the same shape, with in particular a slight hump at approximately 7.147 keV. Similar shapes were obtained for standards of iron oxides like hematite or goethite (Figure 5g) and can be found in the literature for different clays.<sup>40,41</sup>

These results confirm that, in the areas where photoreduction occurs, iron is involved in organic environment, presumably

proteins. Such organic iron has been found in samples D1, D2, and B4, confirming the presence of blood in these samples. At the opposite, only mineral-type XANES spectra have been obtained for sample D3. In this sample, the mineral part is too important to allow unambiguous blood identification with our protocol.

## CONCLUSIONS

Blood identification on cultural heritage artifact is always a challenge due to the small amounts of sample available. However, this kind of study is fundamental for a better understanding of the objects studied and their meaning. In African art, blood is often reported in the elaboration process of artifacts. The results presented in this paper demonstrate, for the first time, that blood was actually used for the making of patina from seven Dogon and Bamana sculptures.

With the use of a three-step approach, the protocol allows us to identify blood using successively TOF-SIMS, SR- $\mu$ FT-IR,  $\mu$ XRF, and  $\mu$ XANES. Thanks to a proper and adequate sample preparation, all analyses can be conducted on the same sample in a noninvasive way, enabling the sample to be used for further analyses.

- (38) Della Longa, S.; Arcovito, A.; Benfatto, M.; Congiu-Castellano, A.; Girasole, M.; Hazeman, J. L.; Lo Bosco, A. *Biophys. J.* **2003**, *85*, 549–558.
- (39) Carugo, O.; Djinovic Carugo, K. *Trends Biochem. Sci.* **2005**, *30* (4), 213–219.
- (40) Pokrovski, G. S.; Schott, J.; Farges, F.; Hazemann, J.-L. *Geochim. Cosmochim. Acta* **2003**, *67* (19), 3559–3573.
- (41) Giuli, G.; Pratesi, G.; Cipriani, C.; Paris, E. *Geochim. Cosmochim. Acta* **2002**, *66* (24), 4347–4353.



This study has demonstrated our approach being suitable for blood identification in cultural heritage objects, but of course it could also be used in other fields of research. It is important to note that TOF-SIMS could be sufficient for the most recent samples and in which heme is not degraded.

In comparison to other identification techniques such as immunological tests, our approach could appear to be less efficient because some samples, such as D3, could be pointed out as not suitable for analysis. Nevertheless, this three-step approach presents the major advantage to avoid false positive results.

#### **ACKNOWLEDGMENT**

Part of this study was realized at ESRF, Grenoble, France (experiment CH-1777). The authors thank C. Naffah, director of the Centre de Recherche et de Restauration des Musées de France (C2RMF) and J.-P. Mohen, director of the collections at the Musée

du Quai Branly, Paris, for their collaboration and support during this project. We also express our gratitude to A. Gaborit and Y. Allain-Nardone, assistant-curator and conservator, respectively, from the Musée du Quai Branly, for their help during the sampling on a great number of precious objects. We are very grateful to J. Castaing from the C2RMF for his support and advice during this project and to J. Degrouard from the Centre Commun de Microscopie Electronique (UMR CNRS 8080) for his assistance in ultramicrotomy preparation. David Touboul is indebted to the Institut de Chimie des Substances Naturelles (CNRS) for a Ph.D. research fellowship.

Received for review May 16, 2007. Accepted September 25, 2007.

AC070993K